^{2}H NMR Studies of Polymer Multilayer Capsules, Films, and Complexes

Blythe Fortier-McGill and Linda Reven*

Centre for Self-Assembled Chemical Structures (CSACS/CRMAA), Department of Chemistry, 801 Sherbrook St. West, McGill University, Montreal, Quebec H3H 2K6, Canada

Received August 25, 2008; Revised Manuscript Received November 17, 2008

ABSTRACT: The chain dynamics of aqueous suspensions of polyelectrolyte complexes, supported multilayers deposited on submicron silica colloids, and hollow capsules were characterized by wide-line ^{2}H NMR spectroscopy (DNMR) as a function of layer number, temperature, and ionic strength. The strong polyelectrolytes, poly(diallyldimethyl ammonium chloride) (PDADMAC) and poly(styrene sulfonate) (PSS) were employed with selective deuteration of the PDADMAC methyl group. DNMR line-shape analyses showed that there is enhanced chain mobility in the systems with excess positive monomer units, that is, supported multilayers and capsules capped with PDADMAC. Selective deuteration of the first, fifth, and ninth layers confirms that the alternation in chain mobility with the capping layer is a through-film effect. Differential scanning calorimetry (DSC)-detected phase transitions were found to occur between 32 and 45 °C for the PSS/PDADMAC complexes, supported multilayers, and capsules. Whereas the glass transitions of bulk-state polymers are detected by DNMR typically 30 to 40° above the DSC-detected T_g, the onset of fast chain motion for the water-saturated polyelectrolyte complexes and supported multilayers coincides with calorimetric transitions.

1. Introduction

The layer-by-layer method (LBL) has been adapted to make polymer microcapsules with applications such as drug delivery agents, microreaction chambers, and carrier systems.[1,2] Colloidal particles are encapsulated via the sequential adsorption of charged or hydrogen bonding polymers, followed by dissolution of the core. These microcapsules display an interesting array of responses to various environments and stimuli. Depending on the particular combination of polymers, the capsules may shrink or swell in reaction to changes in ionic strength, pH, or temperature.[3−6] The response of micron-sized poly(diallyldimethyl ammonium chloride) (PDADMAC) and poly(4-styrene sulfonate) (PSS) multilayer capsules depends on the identity of the final capping layer. The shrinking of PSS-capped versus the expansion of PDADMAC-capped microcapsules upon heating was ascribed to hydrophobic versus electrostatic effects because PSS-capped capsules were found to be essentially charge neutral, whereas PDADMAC capsules were found to have an excess of positive charge.[3] This effect was shown to be independent of the charge of the first layer, and it is attributed to PDADMAC's mobility, which allows it to penetrate the multilayer system more deeply when added.[4] When sufficient thermal energy is added, enough ionic linkages are simultaneously broken to allow for rearrangement of the polymer chains. Because of PSS's limited mobility, its addition to the multilayer systems is limited to the surface, where only slight overcharging can be achieved. The PSS-capped capsule walls are thus hydrophobic, and the driving force for the shrinking of water-suspended capsules is the minimization of the surface potential energy. PDADMAC-capped capsules contain excess positively charged monomer units, and electrostatic repulsion of charges leads to an expansion of the capsules upon heating. DSC-detected phase transitions at the temperature at which the PSS-capped microcapsules shrink were attributed to a type of glass-melt transition.

To assess the dynamic response of polyelectrolyte multilayer capsules at the chain level directly, we have employed wide-line ^{2}H NMR (DNMR) in submicron-sized PSS/PDADMAC capsules. The smaller-sized capsules are required to provide sufficient material for the detection of an NMR signal. This technique allows for selective probing of the chain mobility by depositing the deuterium-labeled polymer for a specific layer. The calorimetry measurements were also extended to aqueous suspensions of the supported multilayers, the complexes, and PDADMAC-capped capsules.

2. Experimental Section

2.1. Materials. Poly(diallyldimethyl ammonium chloride) (PDADMAC, M_w = 200 000−350 000 g/mol), poly(sodium 4-styrene sulfonate) (PSS, M_w = 70 000 g/mol), and other chemicals were purchase from Aldrich. Snowtex silica colloids (nominal diameter 70−100 nm) were provided by Nissan Chemical.

2.2. Synthesis of PDADMAC-d_3. *N*,*N*-Diallyl-methylamine was prepared by adding allylchloride and NaOH to methylamine in a 2:2:1 mol ratio over a period of 2 h at 10−15 °C and refluxing between 60−80 °C for 5 h. Diallyldimethyl ammonium iodide-d_3 was produced by mixing with iodomethane-d_3 in a 1:2 mol ratio in anhydrous methanol at 35 °C under argon overnight. Diallyldimethyl ammonium chloride-d_3 was produced from an ion exchange of diallyldimethyl ammonium iodide-d_3 with silver chloride. Polymerization at an initial monomer concentration of 4.0 mol/L and 323 K was initiated by thermal decomposition of 2,2′-azobis(2-methylpropionamidine)dihydrochloride (2.0×10^{-5} mol/L). The M_w of 110 000 g/mol was determined by static light scattering (SLS) measurements.

2.3. Sample Preparation. To 400 mL of a 4.2 mg/mL PDADMAC, 0.5 M NaCl solution was added 40 mL of a 25 mg/mL colloidal silica suspension. The samples were sonicated and left to stand for 30 min and centrifuged at 16 000 rpm for 15 min, and the supernatant was removed. Milli-Q water (500 mL) was then added, and the solutions were sonicated until there was a complete resuspension. The suspensions were then centrifuged and decanted again to remove any excess polymer. A total of three washings was performed before the addition of the next layer, 400 mL of a 4.2 mg/mL PSS, 0.5 M NaCl solution. Alternating layers of PDADMAC and PSS were added until a total of either 4, 4.5, or 5 bilayers (PDADMAC/PSS) were deposited. Core dissolution was performed by suspending the coated particles in a 0.55 M HF solution and letting it sit overnight. The capsule suspensions were then washed six times with Milli-Q water using the centrifugation

* Corresponding author. E-mail: linda.reven@mcgill.ca.

10.1021/ma801929g CCC: $40.75
Published on Web 12/12/2008

resuspension steps. The 1:1 and 2:1 PDADMAC/PSS complexes were prepared by adding 12.7 and 6.3 mL, respectively, of the 28 mg/mL PSS, 0.5 M NaCl solution to 10 mL portions of the 28 mg/mL PDADMAC-d_3, 0.5 M NaCl solution and diluting to 30 mL. These solutions were vortex mixed overnight, washed three times with Milli-Q water using centrifugations, and redispersed by vortex mixing. Using elemental analysis, it was found that the 1:1 and 2:1 complexes used in the deuterium NMR studies were actually 1.2:1 and 0.8:1 mol ratio, respectively. The 2:1 complex that was prepared for the NDSC analysis used 10 mg/mL polymer solutions, and the elemental analysis showed that the actual ratio was 1.1:1.

2.4. ζ Potential Measurements. Electrophoretic mobilities of the bare and coated silica particles were measured on a microelectrophoresis apparatus Mk II (Rank Brothers, Bottisham, England) and were converted to ζ potentials using the Smoluchowski equation.

2.5. Differential Scanning Calorimetry. DSC measurements were performed using a nanodifferential scanning calorimeter III, model CSC 6300 (Calorimetry Sciences, Lindon, Utah). Temperature scans on degassed solutions were recorded in the range of 5−90 °C with a heating rate of 1.0 K·min^{-1}.

2.6. ^{2}H Nuclear Magnetic Resonance. Spectra were recorded on a Bruker 600 MHz spectrometer with a ^{2}H frequency of 92.12 MHz. A quadrupole-echo sequence (delay−90y−τ −90x−τ −acquisition) was used in the experiment, and the 90° pulse width, 4.2 μs, was with an echo time (τ) of 24 μs. Typically, for the supported multilayers and capsules with the deuterium-labeled PDADMAC-d_3, 32 000 to 68 000 scans were taken for each spectrum, whereas 7200 scans were acquired for spectra of the complexes. For the deuterium-labeled PSS-d_7, 136 000 scans were typically taken for supported multilayers and capsules, whereas 68 000 scans were taken for the complex, and a pulse width of 5.9 μs was used. The complex and capsules with deuterium-labeled PDADMAC-d_3 as the first or fifth layer were washed three times with deuterium depleted water and were finally concentrated in deuterium depleted water. However, the supernatant of these samples still contained a residual D_2O peak because of the very large number of scans required for these dilute samples. Alternatively, to avoid excessive loss of sample, samples in which the ninth layer was deuterated were not washed with deuterium depleted water; instead, the supernatant signal was later subtracted from the FID. It should be noted that it is more precise to wash with deuterium depleted water, although sample is lost during this process, than to subtract the water signal.

2.7. Nuclear Magnetic Resonance Lineshape Simulations. A FORTRAN code provided by Wittebort et al.[7] was modified. We used this program, which includes the effect of finite pulse width and pulse spacing, to simulate the experimental deuterium NMR line shapes of the PDADMAC-d_3 by closely following a procedure developed by Blum et al.[8,9] The simulations were based on an icosidodecahedron, where the vertices were defined as the jump sites (30 sites). Because the provided program was limited to 40 sites, a polyhedron with the largest number of sites with angles closest to that of the methyl group was chosen. Higher priority was given to the number of sites because it was stated by Blum et al. that the probable reason that a 60-site soccer-ball model provided the best fits was because that model came closest to a small jump model.[8,9] The 30-site exchange matrix was designed to allow jumps to occur from a given site to one of its four nearest neighbors. A schematic for the icosidodecahedron and the jump mechanism is shown in Figure 1. Jumps from 0 to sites 1, 2, 3, and 4 were allowed to occur at the given jump rate. All of the jump sites (vertices of the icosidodecahedron) were considered to have equal equilibrium populations. A reduced quadruple coupling constant of 48 kHz was used in the simulation to account for the fast methyl group rotation around its symmetry axis. Although Blum et al. used a 50 kHz reduced quadruple coupling constant, it was found that for our system a 48 kHz quadruple coupling constant fit more accurately.

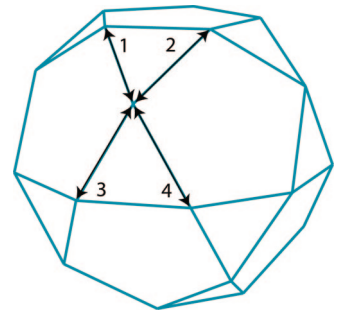

Figure 1. Icosidodecahedron geometry (30 vertices (sites)) used for the simulations. A jump occurs from site 0 to any of the neighboring sites 1, 2, 3, and 4 at the specified jump rate. All sites have equal equilibrium populations.

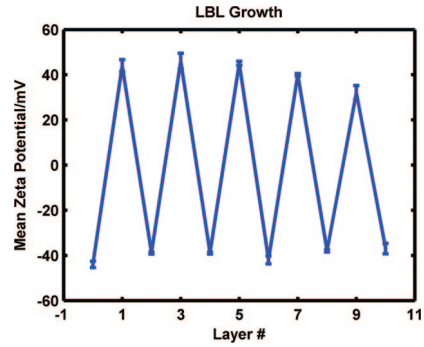

Figure 2. ζ potential measurements as a function of layer number.

A 24 μs pulse spacing and a 4.2 μs pulse width were used for the quadruple-echo pulse sequence in the simulations.

A series of 53 basis spectra were simulated with varying jumping rates from 10 to 1 × 10^{11} jumps/s. A mathematical routine was applied to fit the experimental line shapes to a superposition of the simulated spectra. The weighting factors of each of the simulated spectra were found by finding the minimum of a scalar function of several variables, starting at an initial estimate using Matlab (The Mathworks, Natick, MA). This is generally referred to as unconstrained nonlinear optimization. The absolute values of the variables were taken so that the positive weighting factors of a series of spectra could be obtained.

3. Results and Discussion

3.1. Capsule Preparation. The LBL encapsulation of the silica colloids was monitored by ζ-potential measurements that displayed the expected alternation between negative and positive potentials (Figure 2).

After core dissolution, elemental analysis by TEM showed a large reduction in the Si peak accompanied by the appearance of a sulfur peak due to the presence of PSS. Micron-sized capsules that are more easily imaged by SEM were also prepared to test the protocol for core dissolution. Whereas the submicron-sized capsules remain as spheres and tend to aggregate upon drying, the micron-sized capsules remain more separated and collapse, allowing core dissolution to be visually detected by SEM (Figure 3c,d).

3.2. Effect of the Capping Layer: Dynamic Nuclear Magnetic Resonance Spectroscopy. The dynamic properties of the PSS- versus PDADMAC-capped capsules were first examined. PDADMAC-d_3 that was selectively labeled at the methyl group was used. The energy splitting, $\Delta\nu_Q$, of the quadrupolar interaction that dominates the DNMR spectrum is given by[10]

$$\Delta\nu_Q = \frac{3}{4}\left(\frac{e^2qQ}{h}\right)(3\cos^2\theta(t) - 1) \quad (1)$$

where e^2qQ/h is the quadruple coupling constant and θ is the angle that defines the orientation of the principle EFG component vector, which lies along the C−D bond relative to the magnetic field direction. A distribution of angles, as present in polycrystalline or amorphous samples, generates the so-called deuterium Pake pattern line shape that has a quadruple splitting around 120 kHz in the absence of molecular motion. Motional frequencies that are equal to or greater than the quadruple splitting will average the line shape, leading to the collapse of the Pake pattern to a narrow isotropic peak at sufficiently large reorientation rates and angle distributions. The reorientation of the methyl group about the three-fold symmetry axis changes the width of the powder pattern but not the shape. Expanding the equation for the quadruple splitting yields[10]

$$\langle\Delta\nu_Q\rangle = \frac{3}{8}\left(\frac{e^2qQ}{h}\right)\langle 3\cos^2\delta(t) - 1\rangle\langle 3\cos^2\beta(t) - 1\rangle \quad (2)$$

where the bracket represents the time average and $\delta(t)$ is the angle between the rotating axis and the magnetic field whereas $\beta(t)$ is the angle between the C−D bond and the rotating axis. In the case of a deuterated methyl group where β is equal to 70.5°, the quadruple splitting is reduced by $^1/_3$. Modeling of the motionally averaged deuterium line shape can be used to evaluate the rates of motion as well as reorientation angles quantitatively. Representative simulations of the DNMR spectra are presented in Figure 10.

As seen in Figure 4, qualitative comparisons of the DNMR spectra of capsules with deuterium-labeled PDADMAC at different layers reveal a distinct trend in the chain mobility with the identity of the capping layer.

The DNMR spectra of capsules, where either the first, fifth, or ninth layer is deuterium-labeled with PDADMAC-d_3, are superpositions of a Pake pattern and an isotropic component, reflecting a heterogeneous distribution of chain motion. The PDADMAC-capped capsules have a larger isotropic component, indicating higher chain mobility relative to the PSS-capped capsules. Because the inner, middle, and outer selectively labeled layers all show this trend, the enhanced mobility of the PDADMAC-capped capsules occurs throughout the film. A similar trend for PDADMAC/PSS supported multilayers in the

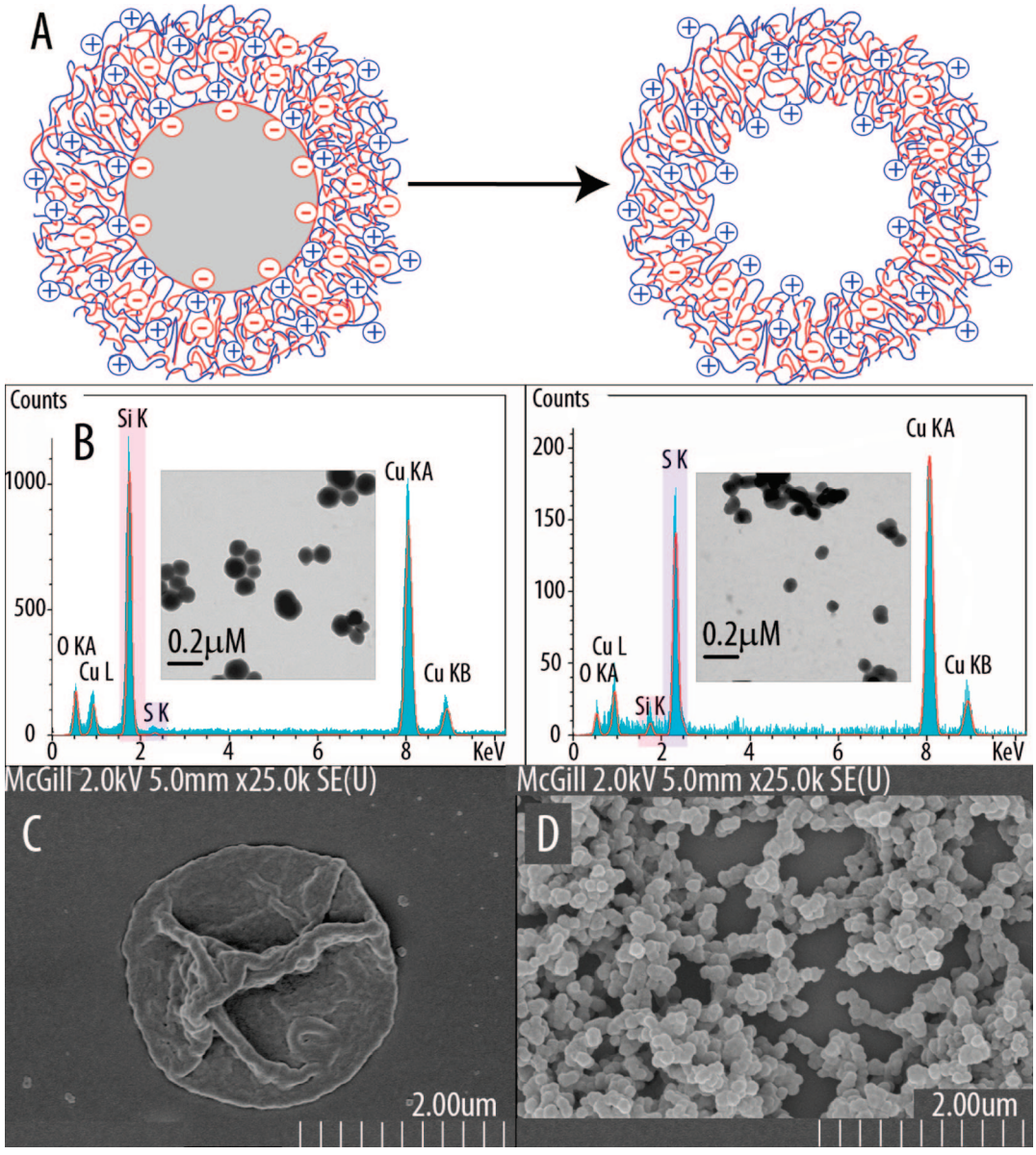

Figure 3. (A) Cartoon depiction of the supported multilayers and the capsules. (B) TEM images and elemental analysis of the supported multilayers and capsules, respectively, with the silica and sulfur peaks highlighted. (C) SEM images of a collapsed 4 μm capsule. (D) Spherical 100 nm capsules.

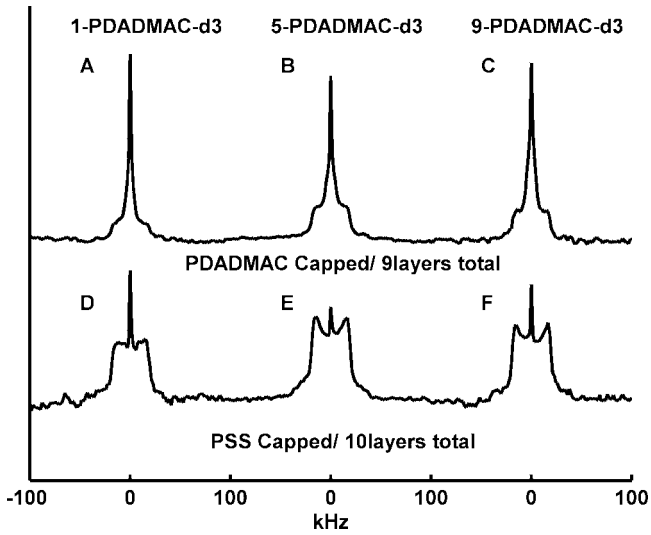

Figure 4. DNMR spectra of the multilayer capsules with (A,B,C) 9 (PDADMAC-capped) versus (D,E,F) 10 (PSS-capped) layers, where the first (1-PDADMAC-d_3) (A,D), fifth (5-PDADMAC-d_3) (B,E), or ninth (9-PDADMAC-d_3) (C,F) layer is deuterium-labeled.

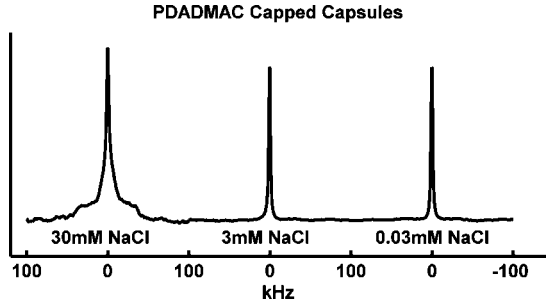

Figure 5. DNMR spectra of the PDADMAC-capped capsules with a total of nine layers, where the first layer is composed of the methyl deuterated PDADMAC-d_3. The capsules are suspended in either 0.03 or 3 mM NaCl, where the capsules are observed to swell, or 30 mM NaCl, where the capsules are observed to shrink.

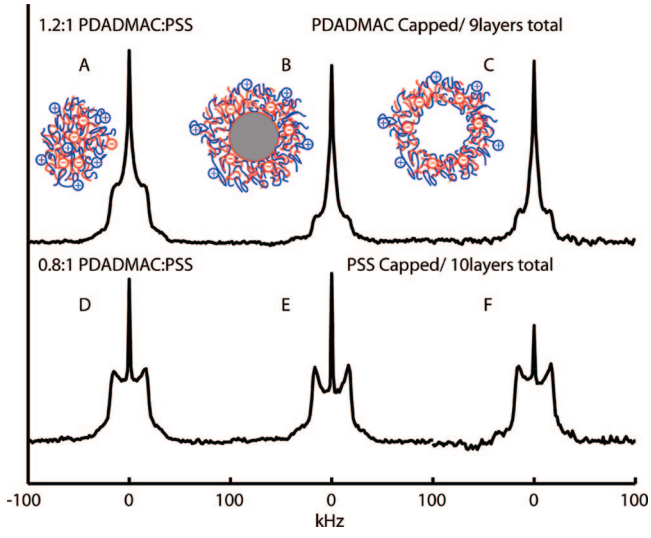

Figure 6. DNMR spectra of aqueous suspensions of the 1.2:1 and 0.8:1 PDADMAC/PSS complexes (A,D) and 9-layer (PDADMAC-capped) (B,C) and 10-layer (PSS-capped) (E,F) supported multilayers (B,E) and capsules (C,F).

dried state was indirectly determined by solid-state ^{1}H MAS NMR experiments to probe the chain mobility via motional averaging of the proton−proton dipolar coupling.[11]

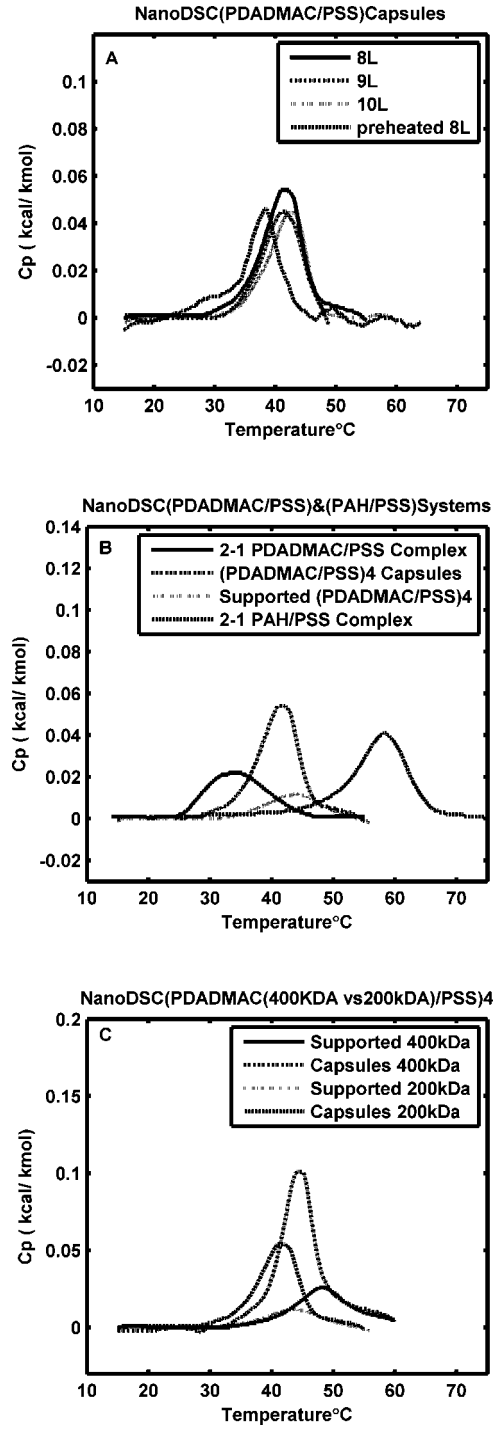

Figure 7. NDSC scans at 1.0 K·min^{-1} of (a) the capsules with 8, 9, and 10 layers and heated 8-layered capsules, (b) the 2:1 PDADMAC3/PSS complex, capsules, and supported films with a total of 8 layers as well as the 2:1 PAH/PSS complex, and (c) the supported multilayers and capsules with a total of 8 layers with either 200−350 kDa PDADMAC or 400−500 kDa PDADMAC.

The isotropic component is assigned to highly mobile PDADMAC segments that are not complexed with PSS and are thus solvated and only associated with small counterions. This assumption is supported by the addition of NaCl to weaken the polycation−polyanion ionic linkages through charge screening. Reversible swelling and shrinking induced by heating PDADMAC-capped capsules to between 40 and 50 °C is observed at 3 and 30 mM NaCl, respectively.[5] This reversible behavior is not observed be means of simple heating and cooling.[3] Capsules with a total number of nine layers show a

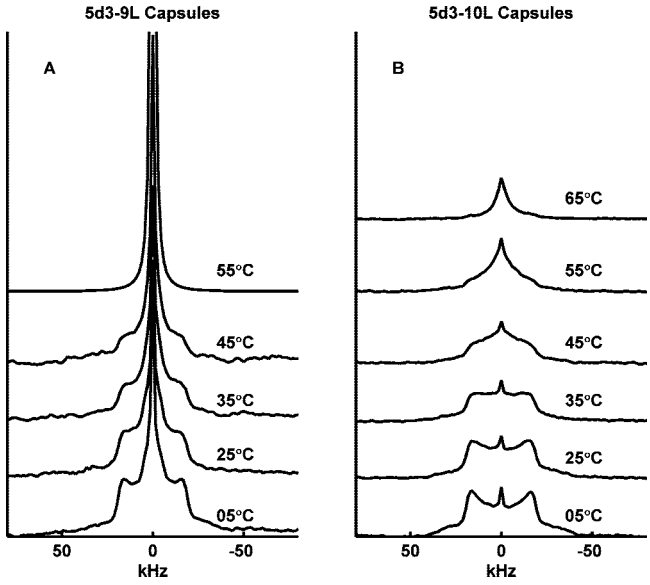

Figure 8. Representative variable temperature DNMR spectra of the (PDADMAC/PSS) capsules with (a) 9 layers (PDADMAC-capped) and (b) 10 layers (PSS-capped), where the fifth layer was assembled using PDADMAC-d_3.

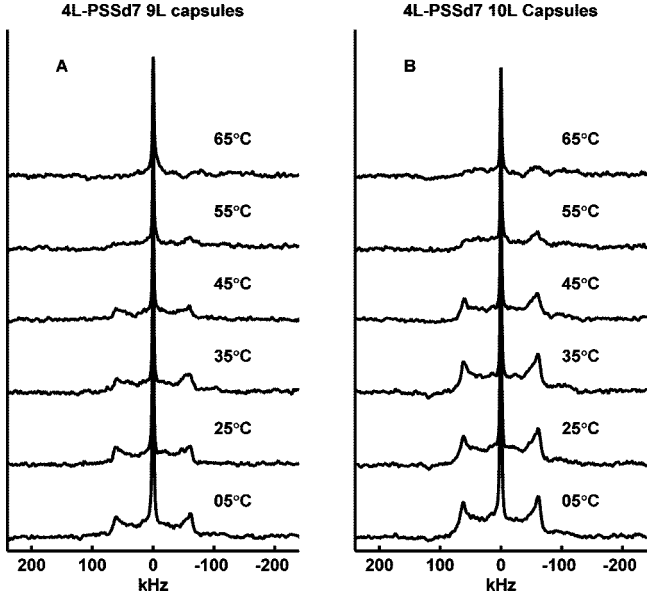

Figure 9. Variable temperature DNMR spectra of the (PDADMAC/PSS) capsules with (a) a total of 9 layers (PDADMAC-capped) and (b) a total of 10 layers (PSS-capped), where the fourth layer was assembled using the fully deuterated PSS-d_7.

complete collapse of the Pake pattern component upon the addition of salt at these ionic strengths (Figure 5). SEM images of the 30 mM NaCl PDADMAC-capped capsules (data not shown) demonstrate that they remained intact, which is in agreement with Kohler et al.[5]

In Figure 6, the DNMR spectra of aqueous suspensions of the complex, the supported multilayers, and the capsules are compared. The systems containing an excess of positively charged monomer units of PDADMAC, that is, the 1.2:1 PDADMAC/PSS complex and the PDADMAC-capped supported multilayers and capsules, have a larger isotropic component that is reflective of a higher chain mobility, demonstrating similar chain dynamics in all three systems.

3.3. Temperature Response: Nano Differential Scanning Calorimetry. Differential scanning calorimetry using a Nano-DSC (NDSC) apparatus was combined with DNMR to examine

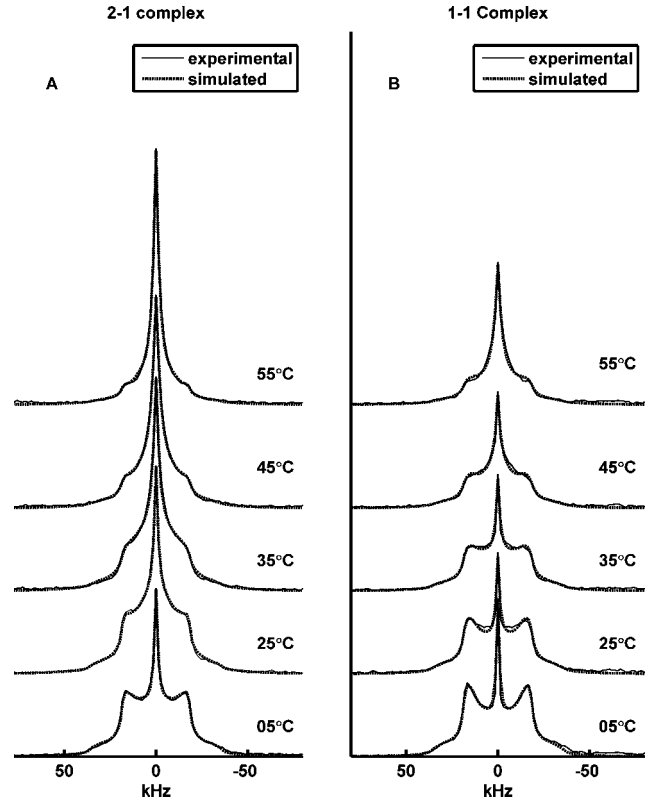

Figure 10. Experimental (—) and simulated (•••) DNMR spectra of (a) the 2:1 complex of PDADMAC-d_3/PSS and (b) the 1:1 complex.

the temperature response of the capsules and related systems. NDSC, which was developed to measure the thermal stability and heat capacity of macromolecules in dilute solutions, was particularly useful in detecting transitions in the aqueous suspensions of the complexes, supported films, and capsules because of its high sensitivity.[12] Micro-DSC measurements have shown that the PSS-capped microcapsules undergo a transition in the temperature range in which the capsules are observed to shrink.[4] However, calorimetric studies of the PDADMAC-capped capsules, aqueous suspensions of the complex, or supported multilayers have not been previously reported.

As seen in Figure 7a, the NDSC measurements of the submicron-sized 8-layered capsules (PSS-capped) as well as the 9- and 10-layered capsules showed transitions in the same 40−45 °C temperature range as that previously reported for the 8-layered microcapsules. When left for a minimum of 24 h, the heated eight-layered submicron capsules have a reproducible transition at 38 °C that is similar to the transition at 35 °C reported in the literature for the heated 8-layered microcapsules (Figure 7a). Furthermore, a transition in the same temperature range as that of the capsules was detected for aqueous suspensions of the PDADMAC/PSS-supported multilayers, whereas the PDADMAC/PSS complex has a transition at a slightly lower and broader temperature range (30−40 °C) (Figure 7b), demonstrating that the transitions are not specific to the hollow capsules and do not strictly arise from surface effects. Instead, the transition temperatures reflect the thermal energy that is required to break the hydrated PDADMAC/PSS ionic linkages.

To test the premise that the strength of the ionic linkages is the main factor in determining the transition temperature, a 2:1 poly(allylamine hydrochloride)(PAH)/PSS complex was examined by NDSC. The transition occurs in a significantly higher transition range (55−60 °C) (Figure 7b). The association of PAH with PSS is known to be much stronger than that of PDADMAC with PSS, producing stiffer supported multilayers that require

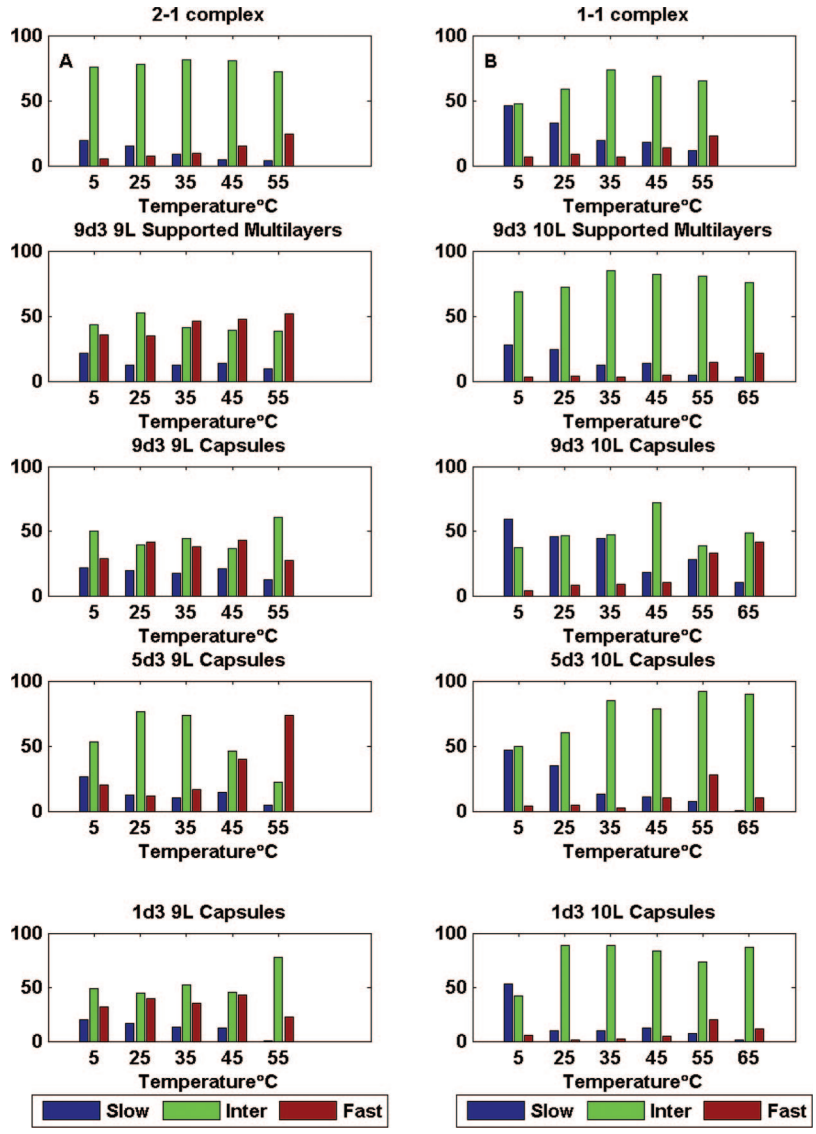

Figure 11. Graphical representation of motional rate distribution grouped into slow, intermediate, and fast regimes for (a) the systems with an excess of the PDADMAC and (b) the systems that are charge balanced.

very high ionic strengths to induce swelling or softening.[13] Likewise, the higher molecular weight of PDADMAC shifts the thermal transitions of the capsules and supported films to a slightly higher temperature range of 45−50 °C (Figure 7c).

3.4. Variable Temperature Dynamic Nuclear Magnetic Resonance. The DSC endotherms reported above are closely correlated with the onset of enhanced chain mobilities, as probed by DNMR spectroscopy. Representative VT DNMR spectra of the capsules are given in Figure 8. Very similar trends are observed for the supported multilayers and capsules. (See the Supporting Information.) For the systems with excess positive PDADMAC monomer units, that is, the 1.2:1 PDADMAC/PSS complex, the PDADMAC-capped capsules, and supported multilayers, the collapse of the broad component consistently commences around 25 °C (Figure 8a). For the systems that are nearly charge balanced, that is, the 0.8:1 PDADMAC/PSS complex and PSS-capped supported multilayers and capsules, the collapse begins at a slightly higher temperature range of 35−45 °C (Figure 8b).

This transition was described by Kohler et al. as a sort of a melt-glass transition whose temperature is a function of composition (i.e., ratio between polyelectrolytes and molecular weight) and wall thickness.[4] The temperature dependence of the DNMR spectra of the capsules and related systems is markedly different from those observed for bulk-state amorphous polymers going through a glass transition. The calorimetric glass transition of bulk solid polymers is associated with sub-hertz motion, whereas NMR probes kilohertz to megahertz motions. Therefore, the NMR T_g, that is, the temperature at which the Pake pattern collapses into an isotropic peak, for bulk amorphous solid polymers is normally 30−40 °C higher than that of the transition detected by DSC measurements.[8] However, the onset of enhanced chain motion of the aqueous suspensions of the capsules, supported multilayers, and complexes as detected by DNMR does not occur at temperatures higher than the calorimetric transitions.

The reported T_g of dry PDADMAC (70 °C)[14] is significantly lower than that recently reported for dry PSS (180 °C)[15] or the dry 1:1 PDADMAC/PSS complex (100 °C). Note that these temperatures may actually be higher because the complete removal of the water, which acts as a plasticizer, is quite difficult. In the case of PDADMAC, the dried state T_g was obtained by extrapolation, and there may be a significant margin of error involved.[16] Likewise, previous work on sulfonated

polystyrene ionomers would indicate a much higher T_g for PSS.[17] Ionomers typically exhibit two glass transitions associated with the organic matrix and the ionic clusters, although these separate glass transitions are difficult to observe by DSC because of phase dimension problems. Whereas the T_g of normal organic polymers is determined by the barrier-to-bond rotation in addition to intermolecular constraints, the ionic interaction strength determines the ionic core T_g, which is typically much higher than that of the matrix. In the case of poly(styrene-*co*-sodium styrene sulfonate) ionomers, the difference between the matrix and cluster glass-transition temperatures was found to be ~120 °C.[17] Water acts as a plasticizer, weakening the ionic interactions, with the T_g of PDADMAC decreasing to ~25 °C when it has a water content of 25 wt %.[14] A similar effect presumably operates in the case of water-saturated polyelectrolyte complexes and supported multilayers, greatly lowering the glass-transition temperatures. When the water-suspended complexes and supported multilayers are heated, the breakage of enough adjacent ionic bonds allows the solvation of the polymer chain segments and a transition from a glassy state to chain motions with frequencies of ≥200 kHz. Thus, the collapse of the Pake pattern coincides with the DSC-detected transition temperature rather than higher temperatures, as normally observed for bulk-state solid polymers in which the chain motional frequencies gradually increase with heating. Upon cooling, the DNMR spectra of the complexes, PSS-capped capsules, and supported multilayers return to their original state (data not shown), whereas the NDSC transition is reproducible only after 24 h. The DNMR spectra of the PDADMAC-capped capsules and supported multilayers contain a larger isotropic component after heating and cooling, indicating that some of the PDADMAC chain segments remain solvated.

3.5. Variable Temperature Dynamic Nuclear Magnetic Resonance of PSS-d_7. To confirm that the DSC endotherms are associated with the onset of chain motion via the breakage of polycation−polyanion linkages, DNMR of samples prepared with perdeuterated PSS-d_7 were studied. Figure 9 shows the DNMR spectra of the PSS-d_7 as the fourth layer within capsules with a total of 9 (PDADMAC-capped) (Figure 9a) and 10 layers (PSS-capped) (Figure 9b). The narrow isotropic component is a contribution of both the D_2O and some solvated chain segments. Note that the signal from D_2O was much larger than that in the case of the PDADMAC-d_3-labeled samples because more signal averaging was required for the broader PSS-d_7 signals. Furthermore, as discussed below, the PSS signal is attenuated because of the chain mobility approaching the intermediate motional regime. Although not as evident as that for the DNMR spectra of PDADMAC-d_3 because of the poor signal-to-noise, the intensity of the Pake pattern of the PSS-d_7 is stronger for the 10-layer samples. The quadruple splitting of PSS-d_7 is $\Delta\nu_o \approx 120$ kHz, whereas in PDADMAC-d_3, the methyl group rotation reduces $\Delta\nu_o$ to ~40 kHz. As the temperature is increased, there is a decrease in the overall intensity of the rigid powder pattern. It is well documented that the intensity of the deuterium Pake pattern decreases when the rate of motion approaches the magnitude of the quadruple coupling constant[18,19] because of destructive interference during the refocusing of the magnetization to produce the quadrupolar echo. As seen in Figure 9a, the Pake pattern contribution vanishes within the same temperature range as that in which the PDADMAC-d_3 Pake pattern collapses into the isotropic peak and is almost completely gone at temperatures of >45 °C. Further heating to increase the motional frequency beyond the intermediate range would presumably lead to a large increase in the intensity of the isotropic peak for the PSS-d_7. Similar trends were observed for PSS-d_7-labeled complexes and supported films.

3.6. Dynamic Nuclear Magnetic Resonance Lineshape Simulations. In addition to the qualitative study of the relative chain motilities that was described in the preceding sections, DNMR line-shape simulations of the PDADMAC-d_3-labeled samples were carried out to quantify the rates of motion surrounding the melt-glass transition. An approach by Blum and coworkers that has been used to examine the motional heterogeneity during the glass transition of bulk amorphous polymers[8] as well as that of surface adsorbed and confined polymers[9] was adapted to our systems. This approach takes into account a large distribution of frequencies by averaging a series of simulated spectra of different jumping rates to fit the experimental spectrum. As described in the Experimental Section, the Wittbort et al. simulation program[7] was modified to simulate the spectra by using nearest neighbor jumps on the vertices of a 30-site icosidodecahedron to mimic small-angle jumps. Figure 10 shows an example of how well the simulated spectra fit the experimental spectra. Because the small jump model has been successfully applied to amorphous polymers,[20] variable echo time line-shape fits were not performed to validate the model used. However, such measurements are especially useful in testing the uniqueness of the model for systems in the intermediate motional regime.

Following Blum's method of simplification, the sets of simulated spectra were grouped together with respect to their motion rates as slow (1.0×10^2 to 1.00×10^4), intermediate (1.1×10^4 to 1.5×10^5), or fast (2.0×10^5 to 1.00×10^{11} jumps/s).[9] The distributions of these jumping rates for different samples as a function of temperature are shown in Figure 11. It can immediately be seen that there is significantly more fast component in the systems in which there is excess PDADMAC or positive charge (Figure 11a) compared with the systems that are essentially charge neutral (Figure 11b), which are more dominated by the intermediate component. There is also a significant change in the distribution of motion from 35 to 45 °C for the capsules that coincides with the NDSC transition (40−45 °C).

4. Conclusions

At the chain level, the dynamic properties of aqueous suspensions of PDADMAC/PSS complexes, supported multilayers deposited on colloidal silica, and hollow microcapsules are very similar. The chain mobility is heterogeneous and consists of a glassy component due to segments with strong polyanion/polycation linkages and a mobile component arising from solvated segments that are weakly associated with small counterions. The proportion of mobile chain segments is higher in the systems with excess positive monomer units, that is, the PDADMAC-capped supported multilayers and capsules. However, selective DNMR spectra of the inner, middle, and outer PDADMAC layers show that this mobile component is not only associated with the surface but also distributed throughout the multilayer film. The DNMR spectra of deuterated PSS further support this picture of an overall increase in chain mobility in the systems with excess positive monomer units. Calorimetric phase transitions, described as glass/melt transitions, occur in a similar temperature range as that of aqueous suspensions of the PSS/PDADAMAC complexes, supported multilayers, and hollow microcapsules. The transition temperatures, which are far lower than any T_g of the bulk dry complexes, are primarily determined by the strength of the hydrated ionic linkages rather than surface effects. These transitions are associated with the onset of fast chain motion due to the simultaneous breaking of enough ionic linkages to allow for solvation and rearrangement of the chain segments.

Acknowledgment. Dr. Violeta Toader (CSACS/CRMAA) synthesized the PDADMAC-d_3. We also acknowledge the assistance of Drs. Fred Morin (McGill) and Cedric Malveau (U. Montreal) with the NMR spectroscopy. Access to the Nano DSC apparatus was generously provided by Professor Anthony Mittermaier (McGill). We thank Professors C. T. Yim (Dawson College, Montreal) and Frank Blum (Missouri U. of Science and Technology) for valuable advice regarding the line-shape simulations as well as Lynda Cockins (McGill) for assistance with the Matlab fitting functions.

Supporting Information Available: DNMR spectra of capsules, supported multilayers, and complexes. This material is available free of charge via the Internet at http://pubs.acs.org.

References and Notes

(1) Johnston, A. P. R.; Cortez, C.; Angelatos, A. S.; Caruso, F. *Curr. Opin. Colloid Interface Sci.* **2006**, *11*, 203.
(2) Donath, E.; Sukhorukov, G. B.; Caruso, F.; Davis, S. A.; Möhwald, H. *Angew. Chem., Int. Ed.* **1998**, *37*, 2201.
(3) Köhler, K.; Shchukin, D. G.; Möhwald, H.; Sukhorukov, G. B. *Phys. Chem. B* **2005**, *109*, 18250.
(4) Köhler, K.; Möhwald, H.; Sukhorukov, G. B. *J. Phys. Chem. B* **2006**, *110*, 24002.
(5) Köhler, K.; Biesheuvel, P. M.; Weinkamer, R.; Möhwald, H.; Sukhorukov, G. B. *Phys. Rev. Lett.* **2006**, *97*, 188301.
(6) Sukhorukov, G. B.; Antipov, A. A.; Voigt, A.; Donath, E.; Möhwald, H. *Macromol. Rapid Commun.* **2001**, *22*, 44.
(7) Wittebort, R. J.; Olejniczak, E. T.; Griffin, R. G. *J. Chem. Phys.* **1987**, *86*, 5411.
(8) Metin, B.; Blum, F. D. *J. Phys. Chem.* **2006**, *125*, 054707.
(9) Okuom, M. O.; Metin, B.; Blum, F. D. *Langmuir* **2008**, *24*, 2539.
(10) Ulrich, A. S.; Grage, S. L. ^{2}H NMR. In *Solid State NMR of Polymers*; Ando, I., Asakura, T., Eds.; Elsevier: Amsterdam, 1998; p 190.
(11) McCormick, M.; Smith, R. N.; Graf, R.; Barrett, C. J.; Reven, L.; Spiess, H. W. *Macromolecules* **2003**, *36*, 3616–3625.
(12) TA Instruments, New Castel, Delaware.
(13) Jaber, J. A.; Schlenoff, J. B. *Langmuir* **2007**, *23*, 896.
(14) Yeo, S. C.; Eisenberg, A. *J. Macromol. Sci. Phys.* **1977**, *B13*, 44.
(15) Imre, Á. W.; Schönhoff, M.; Cramer, C. *J. Chem. Phys.* **2008**, *128*, 134905.
(16) A. Eisenberg, personal communication.
(17) Eisenberg A.; Kim J.-S. *Introduction to Ionomers*; Wiley: New York, 1998; p 78.
(18) Lee, Y. J.; Murakhtina, T.; Sebastiani, D.; Spiess, H. W. *J. Am. Chem. Soc.* **2007**, *129*, 12406.
(19) Wittebort, R. J.; Usha, M. G.; Ruben, D. J.; Wemmer, D. E.; Pines, A. *J. Am. Chem. Soc.* **1988**, *110*, 5668.
(20) Metin, B.; Blum, F. D. *J. Chem. Phys.* **2006**, *124*, 054908.

MA801929G